Examining the Energy Imbalance of Eddy-Covariance Measurements in a Tidal Wetland

Author: Angèlica Busquets Rubiés, angelica.arbre@gmail.com
Director: Ariane Arias Ortiz, Ariane.Arias@uab.cat, *Departament de Física, Universitat Autònoma de Barcelona, Carrer dels Til·lers, 08193 Bellaterra, Spain.*
Co-Director: Tianxin Wang, cawang@berkeley.edu, *Department of Environmental Science, Policy, and Management, University of California, Berkeley, 130 Mulford Hall, Berkeley, CA 94720, United States.*
University Supervisor: Mireia Udina Sistach, mudina@meteo.ub.edu
Departament de Física Aplicada, Universitat de Barcelona, C/Martí i Franquès 1, 08028 Barcelona, Spain.

Abstract: The energy balance of the Earth's surface is crucial for understanding biosphere-atmosphere interactions. However, the energy imbalance observed in eddy-covariance measurements indicates that our understanding and estimation of ecosystem dynamics remains incomplete. This issue is especially important for wetlands, which have an important role in global climate processes and exhibit the highest imbalances. In this study, we investigated the energy balance closure (EBC) in a restored tidal wetland. The EBC ratio before tidal restoration was 0.9, contrasting with a poor closure of 0.22 after tidal restoration. We applied filters based on friction velocity ($u*$), wind direction and zenith angle, as well as accounting for soil heat storage. These filters improved closure before tidal restoration, but did not for the period after tidal restoration. Daily averaged fluxes enhanced closure up to 54%, suggesting the role of water storage, lateral water heat advection and an influence from large-scale eddies. Analysis of the Bowen ratio and the Priestley-Taylor parameter suggests influence of lateral heat advection after tidal restoration. Future research should include the challenging computations of these energy terms. These insights contribute to a deeper understanding of energy exchanges in tidal wetland environments and underlines important terms that should be taken into account, thereby aiding climate change studies and the management of wetland restoration.

I. INTRODUCTION

The surface energy balance (SEB) is a crucial element for understanding the interactions between the biosphere and the atmosphere as well as the dynamics of our planet's climate (*Liu et al.* 2017; *Mauder et al.* 2020). SEB is commonly expressed with the energy balance closure (EBC) ratio between the turbulent fluxes and the net available energy:

$$EBC = \frac{H + LE}{Rn - G} \tag{1}$$

where H and LE represent the sensible and latent heat fluxes, respectively, Rn denotes the net radiation and G accounts for the ground heat flux (*Liu et al.* 2017). They are all defined positive when energy is transferred away from the surface, except for the net radiation, which is considered positive when the surface gains energy. These fluxes arise from differential horizontal and vertical heating driving buoyancy as well as from the biological, geological and meteorological conditions of the ecosystem, all of which results in eddies and turbulence within the atmosphere boundary layer.

Our understanding of the energy terms relies on observations from eddy covariance (EC) flux measurement towers and flux measurement networks such as FLUXNET (*Stoy et al.* 2013). The EC method, a widely employed technique, measures the energy and trace gases exchange between the surface and the atmosphere via the covariance between fluctuations in vertical wind velocity and the scalar of interest (*Baldocchi* 2003).

Theoretically, the EBC ratio on the surface should be equal to 1, meaning an equilibrium between energy inputs and outputs on the surface. However, as it has been heavily discussed in the literature since the late 1980s (*Mauder et al.* 2020; *Foken* 2008), in most cases the net available radiation is found to be larger than the sum of the turbulent fluxes of sensible and latent heat, and an underestimation of turbulent fluxes is argued as the reason for the problem (*Foken* 2008). The total contribution of neglected effects and uncertainties is considered as the imbalance or residual (*Mauder et al.* 2020).

Studying data from numerous sites, *Stoy et al.* (2013) found an average EBC ratio of 0.84 ± 0.20. The best average closures were observed in evergreen broadleaf forests and savannas (0.91–0.94), while the worst average closures were observed in crops, deciduous broadleaf forests, mixed forests and wetlands (0.70–0.78).

These findings raise concerns within the micrometeorology community regarding the quality and usability of eddy-covariance measurements in surface flux models (*Foken* 2008; *Liu et al.* 1999; *Twine et al.* 2000).

Factors that have been found to be important for the closure of the SEB (*Foken* 2008) are, on one hand, the additional storage terms. On the other hand, better results for a wider averaging time or area-averaged fluxes suggest that bigger-scale eddies may influence the EBC.

These larger turbulence structures also affect the footprint and are related to the heterogeneity of the land, which may provoke secondary circulations with its advections which lead to an increase in the imbalance (*Mauder et al.* 2020). Accurately measuring the divergence or convergence term attributed to advection in flat terrain remains a challenge.

Several questions remain yet to be answered to be able to fully understand the energy surface fluxes, and although a complete closure can occur at certain sites, the energy balance at several flux sites worldwide remains unclosed (*Stoy et al.* 2013). Wetland ecosystems exhibit the poorest EBC among FLUXNET sites (*Cui et al.* 2019). However, the reasearch conducted on the energy fluxes of these ecosystems is still limited and an exhaustive analysis of the underlying interactions among flora, fauna, and heat stored in coastal wetlands is still lacking (*Piccolo* 2019). Wetland's energy budget is not only influenced by energy storage in soil, but also in water (*Pokorný et al.* 2010), which complicate energy balance terms. Tidal wetlands face even greater challenges due to strong horizontal fluxes, particularly those driven by water movement (*Moffett et al.* 2010; *Piccolo* 2019).

Covering about 6.4% of Earth's surface (*DAC* 1996), wetlands globally hold 20-30% of the estimated 1.500 Pg of soil carbon (C) (*Lal* 2007). However, land use changes have caused a 50% global loss of wetlands (*Davidson* 2014), impacting large pools of stored C (*Pendleton et al.* 2012). Understanding wetland energy fluxes is critical due to their capacity for carbon dioxide (CO_2) sequestration as photosynthesis exceeds oxygen-inhibited respiration in their waterlogged soils, potentially aiding climate change mitigation (*Mitra et al.* 2005). Energy dynamics are vital to ecosystem analysis, due to their influence on the hydrologic cycle and biogeochemical processes.

This study aims to address how does tidal restoration impact the EBC of a wetland. Our hypothesis is that tidal restoration will initially worsen the EBC due to changes in energy dynamics. However, we expect that the EBC will improve after applying adequate filters and accounting for heat storage terms. The investigation seeks to describe the impact of flooding and tides on each component of the energy budget and to understand the underlying causes of the ecosystem's energy imbalance.

II. METHODOLOGY

A. Site description

The restored wetland site is located within the Hill Slough Wildlife area next to Suisun City, California, USA (38.24^o N, 122.02^o W), at an elevation of 1.113 m NAVD88, and it is part of the AmeriFlux network (*Arias-Ortiz et al.* 2024).

The site features a marsh ecosystem with a Mediterranean climate, a mean annual temperature of 15.6 ^{o}C and a mean annual precipitation of 450 mm. The prevailing wind direction at the site is from the southwest (see Appendix A).

In October 5, 2021, the site underwent a tidal restoration conducted by Ducks Unlimited, a wetland conservation organization, covering an area of 2.6 km^2. Energy and gas flux measurements, along with meteorological data collection, began on March 12, 2021, nearly seven months prior to the restoration. At that time, the site was characterized by a seasonal wetland dominated by sparse pickleweed (*Salicornia pacifica*) and various salt grasses.

Following the restoration, vegetation remains minimal, resulting in sparse coverage. The site is inundated twice daily due to semi-diurnal tides, and the soil remains continuously saturated with water. The mean tidal range is 1.27 meters, and salinity levels range between 0.5 ppt in the winter and 12 ppt during the summer months.

B. Atmospheric Exchanges in Wetland Ecosystems

1. *Eddy Covariance Method*

At any given moment, an eddy moves an air parcel either downward or upward at a certain speed, with each air parcel carrying unique characteristics such as gas concentration, temperature, and humidity. The essence of the EC method is that the various vertical fluxes can be found as the covariance between vertical velocity, w', and the variable of interest (*Burba and Anderson* 2010).

Wind velocity components can be decomposed into their mean velocity $\overline{u}$ and their fluctuation u' around the mean, a process known as Reynolds decomposition: $u = \overline{u} + u'$, where $\overline{u'} = 0$ (*Reynolds* 1895). Rotating eddies generate vertical flows, w'. Typically, for the horizontal flow $\overline{u} >> u'$ and for the vertical flow $\overline{w} << w'$.

As enumerated in *Burba and Anderson* (2010), several assumptions are necessary for the effective application of the EC method. These include a steady-state condition; all turbulent eddies being advected by the mean flow without changing their properties (Taylor's hypothesis); horizontal homogeneity (thus neglecting horizontal advection and flux divergence/convergence); negligible mean vertical wind speed ($\overline{w} \approx 0$); complete measurement of all eddies; measurements at a point being representative of an upwind area; an adequate footprint; and zero air density fluctuations.

The EC method achieves the highest accuracy under conditions where temperature, wind, and humidity exhibit temporal stability, alongside uniform vegetation covering flat terrain (*Baldocchi* 2003).

Expressions for the sensible heat flux, latent heat flux and ground heat flux (Wm^{-2}) are, respectively:

$$H = \rho C_p(\overline{w'T'}) \; ; \; LE = \rho L_v(\overline{w'q'}) \; ; \; G = -C_l\frac{\partial T_s}{\partial z} \quad (2)$$

where ρ ($kg{\cdot}m^{-3}$) is the air density, C_p ($Jkg^{-1}K^{-1}$) is

the air heat capacity, $\overline{(w'T')}$ $(ms^{-1}K)$ the covariance between the fluctuations of vertical wind velocity and temperature, L_v (Jkg^{-1}) is the latent heat of vaporization of water, $\overline{(w'q')}$ (ms^{-1}) denotes the covariance between the fluctuations of vertical wind velocity and specific humidity (*Stull* 1988), C_l $(Wm^{-1}K^{-1})$ is the soil thermal conductivity, T_s (K) is the soil temperature and z (m) is the soil depth (*Kimball et al.* 1976).

C. Instrumentation

The EC flux tower at Hill Slough was equipped with a three-dimensional ultra-sonic anemometer (Windmaster Pro, Gill Instruments, Lymington, UK) for measuring wind velocity and virtual temperature fluctuations. Net radiation was measured using a net radiometer (NR01 Net Radiometer, Hukseflux, Delft, the Netherlands), while ground heat flux was determined using soil heat flux plates (HFP01 Soil Heat Flux Plate, Hukseflux, Delft, the Netherlands). Temperature and relative humidity of the air were monitored using HMP155A, Vaisala, Inc., Finland, and soil and water temperature was measured by a profile of copper-constantan thermocouples. For a detailed list of all sensors used, please refer to *Berkeley Biometeorology Lab*.

These EC flux tower instrumentation provide high-frequency, 20 Hz, continuous measurements of temperature, water vapor, CO_2 and CH_4 concentrations, along with three-dimensional wind speed measurements, to quantify the net exchange of trace gases and sensible and latent heat between the marsh vegetation and the atmosphere (fast system) (*Baldocchi* 2003). These measurements are averaged over 30-minute intervals, while other meteorological data is collected directly every 10 seconds and is later aggregated in 30 minutes averages (slow system).

D. Data processing

The most common method for computing energy balance involves comparing the half-hourly sums of the LE and H values against half-hourly available energy values and using the slope of the linear regression as an estimate of the closure (*McGloin et al.* 2018). A slope of 1 and an intercept of 0 indicate a perfect energy balance.

Before obtaining analysis-ready fluxes, several processing steps are necessary. For each 30-minute averaging interval, wind speed measurements are rotated into the mean wind direction ($\overline{u}$), ensuring that the mean wind speeds in the other two dimensions ($\overline{v}$ and $\overline{w}$) are zero. To account for air density fluctuations, the Webb–Pearman–Leuning correction is applied to gas fluxes measured with open path sensors (*Webb et al.* 1980). Other corrections include despiking data, accounting for time lags between the sonic anemometer and gas analyzer, and applying calibrations (*Foken* 2008; *Schedlbauer et al.* 2011).

Certain conditions like low fluxes, calm winds, unstable atmospheres, divergence, and convergence can lead to unreliable data. Quality control is crucial for accurate data, involving removing data affected by instrument issues, unsuitable environmental conditions for the EC method, heavy precipitation, and non-stationary periods. This process varies based on the site and instrument (*Burba and Anderson* 2010). As a result, another essential step in EC data processing is gap-filling using artificial neural networks (ANN), although for the evaluation of EBC for this study we used not gap-filled clean data.

To accurately compare energy fluxes before and after the restoration, and to minimize the influence of seasonal variations on the results, we selected data for the EBC analysis that ranges from March 12 to September 30 of 2021, for the period before tidal restoration, and the same dates of 2022 for the interval after tidal restoration.

To analyze the energy imbalance of the tidal wetland, the following specific data analysis was conducted:

1. *Filtering*

Since the restored wetland is located southwest of the tower, only fluxes between 180^o and 270^o were taken into account to ensure flux footprints originate from the ecosystem of interest.

On the other hand, a threshold of 0.2 m/s for the friction velocity $u*$, a crucial parameter in EC measurements that can be calculated as $u*^4 = (\overline{u'w'})^2 + (\overline{v'w'})^2$, was set up based on when nighttime CO_2 fluxes became independent of $u*$ (*Eichelmann et al.* 2018). Low $u*$ values can indicate insufficient turbulence, which affects the reliability of flux measurements.

Finally, we separated nighttime and daytime data, focusing our energy balance closure analysis on daylight hours. Nighttime data require special handling due to conditions such as low wind speeds, stable stratification, and insufficient turbulence. These factors can lead to non-stationary periods, advection, and a significant increase in the footprint, potentially causing the tower to record fluxes outside the intended area.

2. *Heat storage term*

The ground heat flux is measured 2 cm below the surface. The soil heat storage in the layer between the surface and the ground heat flux sensor at 2 cm, Q_{soil} (W/m^2), can also be taken into account in the energy balance as it may have a significant influence on the residual (*Heusinkveld et al.* 2004). Soil storage can be determined as:

$$Q_{soil} = d \cdot C_s \cdot \frac{\partial T}{\partial t} \tag{3}$$

where d is the soil thickness in cm, T is soil temperature (^oC), t is the time and C_s is the heat capacity of the moist soil ($Jg^{-1}K^{-1}$) (*Liu et al.* 2017).

Heat capacity of moist soil can be found as $C_s = rb \cdot C_d + VWC \cdot \rho_w \cdot Cw$, where rb represents the bulk density (kgm^{-3}), C_d the heat capacity of dry soil ($Jkg^{-1}K^{-1}$), VWC the volumetric water content on the top layer of the soil (%), ρ_w (kgm^{-3}) water density, and C_w ($Jkg^{-1}K^{-1}$) the heat capacity of water.

The expression for water storage is analogous to that for soil storage but with VWC set to 1, bulk density considered as zero and $d = d_w$ is used as water thickness.

For the water storage term calculation, water volume was divided into three layers: from the surface to 8 cm, from 8 cm to 32 cm, and from 32 cm to the water level height. This approach was used because we had temperature data for these specific depths, where the thermocouples were located, and it also allows for more accurate tracking of the storage term.

The air heat capacity is small compared with that of the soil and water (*Liu et al.* 2017).

3. *Calculation of key parameters*

For the purpose of analyzing the dataset, we computed the following parameters:

- The stability parameter is defined as $\zeta = (z-d)/L$, where z is the measurement height, d is the zero-plane displacement height, and L is the Monin-Obukhov length. L indicates the height above the surface at which the production of turbulent energy from buoyancy dominates over mechanical shear production of turbulence (*Stull* 1988).

  ζ characterizes the stability state of the boundary layer: $\zeta < 0$ indicates inestability, $\zeta > 0$ indicates stability and $\zeta \sim 0$ indicates neutral conditions (*Foken* 2017).

- The Bowen ratio is defined as $\beta = \frac{H}{LE}$, and it is a useful indicator of an ecosystem's energy contributions to the regional climate. Usually, wetlands have the lowest β of terrestrial ecosystems (*Lafleur* 2008).

- The Priestley-Taylor parameter is indicated as the $\alpha = LE/LE_{eq}$ ratio, relating latent heat flux with equilibrium latent heat flux (*Priestley and Taylor* 1972).

III. RESULTS

In this section, we present the results of the study. Please refer to section IV for a discussion of these results.

A. Meteorological conditions

To assess the meteorological similarity of the years included in the analysis, we examined the mean value of air temperature, which was (18.16 ± 0.07) ^{o}C for the period before tidal restoration and (18.52 ± 0.06) ^{o}C after tidal restoration, a very similar value. The mean value of net radiation increased from (147 ± 3) W/m^2 before tidal restoration to (174 ± 3) W/m^2 after tidal restoration. Additionally, total precipitation amounts were 11.43 mm and 50.10 mm for the before and after tidal restoration periods, respectively. Water level rose from below the surface to (0.203 ± 0.002) m on average after tidal restoration.

Refer to Appendix B for the evolution of air temperature, soil temperature at 0 cm (TS), outgoing longwave radiation (LW), and incoming radiation. After tidal restoration, the deviation in TS and LW is smaller than before, thanks to water's stabilizing effect.

B. Evolution of the energy budget terms

Following the wetland tidal restoration, there was a remarkable shift in energy dynamics (Figure 1). Prior to restoration, H dominated, reaching daily averages maximum levels of 165.62 W/m^2, while LE remained low at 58.42 W/m^2. However, this dynamic flipped after tidal restoration. H maximum value significantly reduced to 72.47 W/m^2, and LE became the predominant component at 258.45 W/m^2. Peak values of turbulent fluxes were recorded during June and July.

Throughout the average daily cycle, beofre tidal restoration, all fluxes reached their maximum at midday, apart from G, which peaked later in the afternoon (Figure 1a). All fluxes were negative at nighttime. After restoration, LE peaked around 15h, and both turbulent fluxes remained positive throughout the entire day.

The energy imbalance increased dramatically after tidal restoration, going from a maximum of 43.47 W/m^2 at 10:00 (Pacific Standard Time, PST) to a maximum of 408 W/m^2 at 11:30 (PST), nearly ten times higher than previously (Figure 1).

C. Impact of filters and heat storage on EBC ratio

Prior to restoration, the EBC ratio was close to one (Figure 2a), characterized by a slope of 0.9 and a high R^2 of 0.97. This indicates an almost balanced state between incoming and outgoing energy fluxes within the study area.

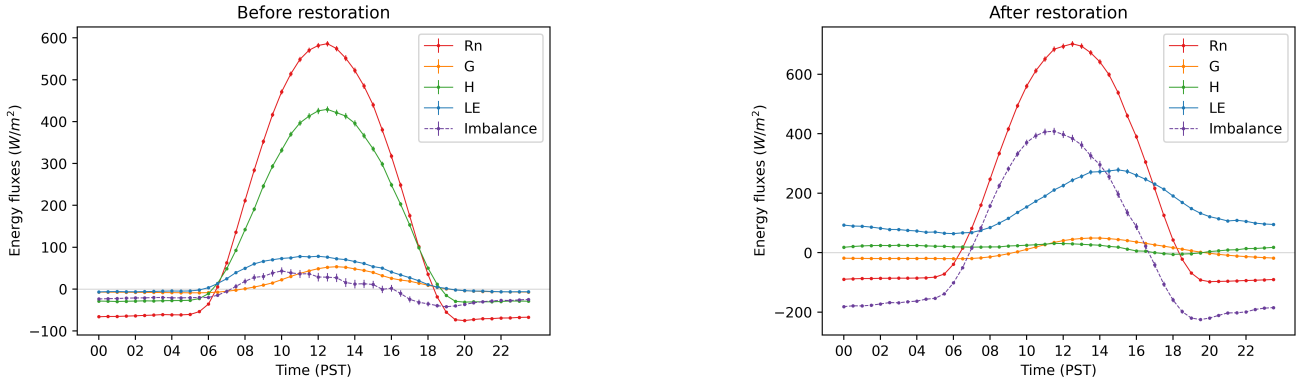

(a) (b)

Figure 1: Diurnal variations in the energy balance components when the site was dry (a) and after tidal restoration (b)

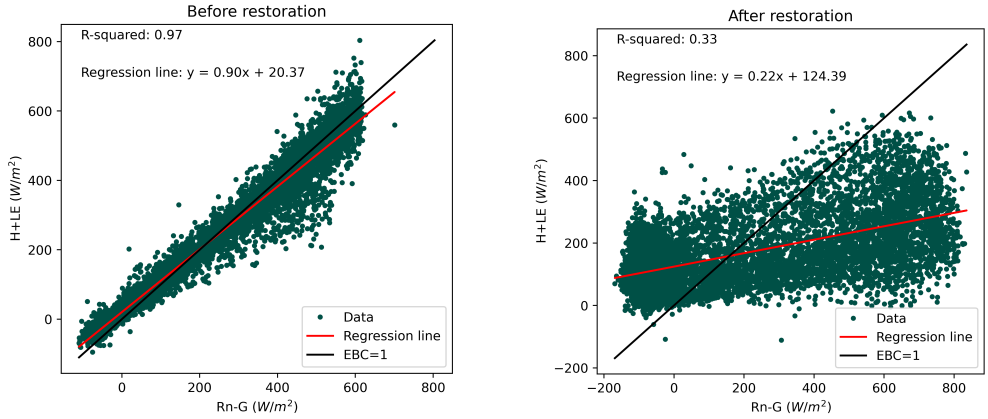

(a) (b)

Figure 2: Relationships between half-hourly data turbulent heat flux ($H + LE$) and available energy ($Rn - G$) before (a) and after (b) restoration.

(a) (b) (c)

Figure 3: Relationships between half-hourly data turbulent heat flux and available energy before (a) and after (b) restoration. (c) also takes into account water heat storage in two layers, (0-8 cm) and (0-Water Level).

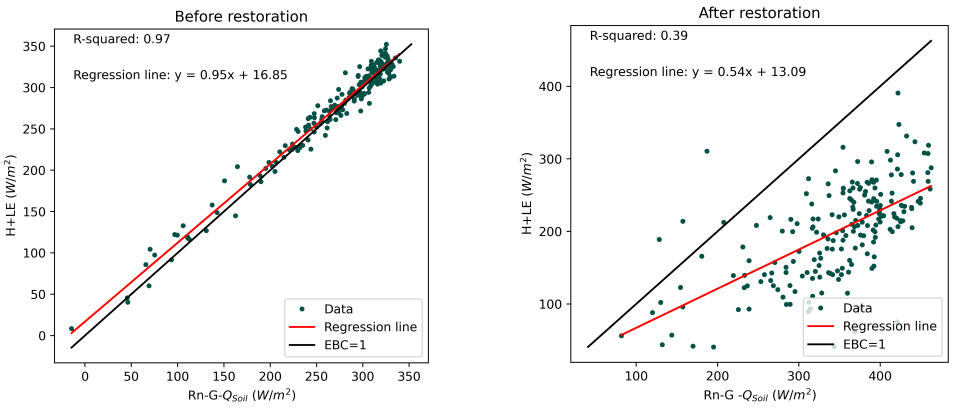

(a) (b)

Figure 4: Relationships between daily averaged turbulent heat flux and available energy before (a) and after (b) restoration.

Following restoration, however, the slope significantly decreased to 0.22, accompanied by a reduced R^2 of 0.33 (Figure 2b), indicating a very poor energy closure.

After filtering the dataset by excluding $u*$ values lower than 0.2 m/s, nighttime data, EBC ratios lower than 0, and constraining the wind direction to our desired area of study, the EBC ratio before tidal restoration showed an improvement, EBC= 0.92. Despite that, applying these filters after tidal restoration reduced EBC to 0.21.

By incorporating the soil heat storage, Q_{soil}, EBC before tidal restoration increased to 0.95 (Figure 3a) and the intercept showed a slight improvement. However, after tidal restoration, the EBC slope marginally increased to 0.23 and it further scattered the data (Figure 3b).

Water heat storage was also added in Figure 3c. Considering only water levels up to 8 cm, the EBC improves with this storage term up to 36%. However, due to the inconsistent results when considering all water column, we have not included it in the further calculations.

D. Impact of daily averaged fluxes in EBC ratio

The EBC improved significantly when moving from half-hourly to daily averaged data after tidal restoration, reaching a slope of 0.54, a considerably improved R^2 value and a much lower intercept Figure 4. This improvement was not observed for the period before tidal restoration, where the original data already reflects a high degree of closure.

E. EBC ratio dependence on meteorological variables

As it is shown in Figure 6, the EBC ratio typically showed values lower than 1, with notable deviations observed at the beginning and end of the day when the zenith angle approached 90 degrees.

We conducted a correlation analysis and, to avoid interference of the very scattered data at sunrise and sunset, we excluded data corresponding to a zenith angle higher than 70 degrees. Variables that showed a relatively high correlation with the EBC ratio are shown in Figure 5. We found a positive correlation between the EBC ratio and LE, $u*$, $\overline{u}$. Figure 5 also indicates that the energy imbalance was higher with lower values of net radiation.

Figure 6 shows us that EBC was worse under neutral stability conditions (where the stability parameter (ζ) approaches 0), which also corresponds to higher zenith angles. Additionally, higher friction velocity was associated with more neutral stability conditions. Sensible heat flux and the Bowen ratio were positive at unstable conditions, negative at stable conditions and notably higher during neutral stability conditions (figures not shown).

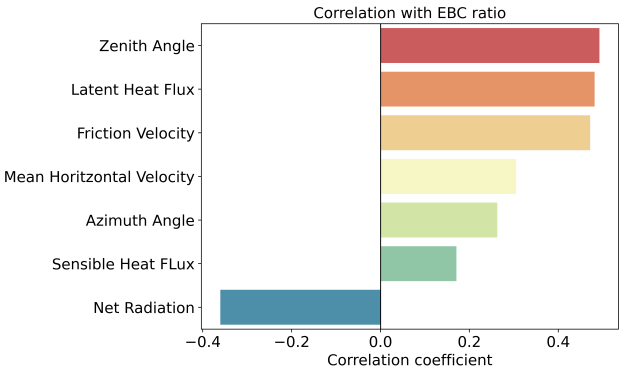

Figure 5: Correlation coefficient between EBC ratio and various meteorological variables.

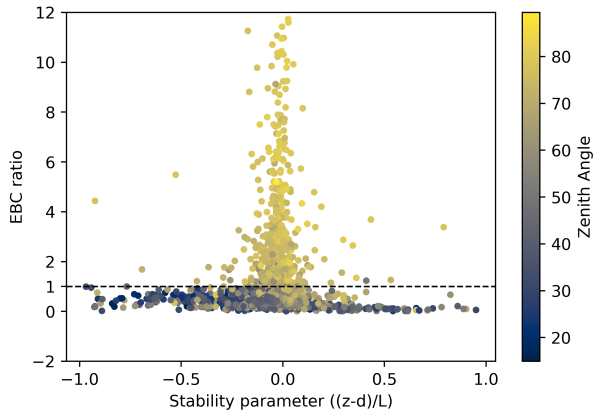

Figure 6: Effect of the stability parameter ((z-d)/L) on the EBC ratio after restoration. Very high values of the stability parameter and EBC ratio have been partially cropped out by the zoom scale, so the plot represents 76% of the dataset.

After tidal restoration, an increase in negative Bowen ratios values was observed, rising from 8.41% to 30.49%. As represented in Figure 7a, positive Bowen ratios aligned more closely with the EBC=1 line compared to negative values. Specifically, the EBC ratio with only positive Bowen ratios was 0.27, whereas with only negative Bowen ratios it was 0.13, with an associated R^2 value of 0.1.

Figure 7b shows us how the majority of Priestley-Taylor parameter values (66.59%) were higher than 1.26.

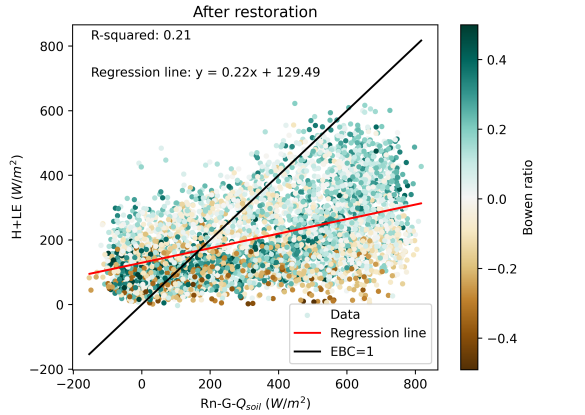

(a)

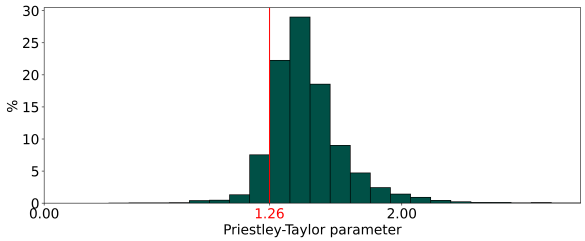

(b)

Figure 7: Relationships between half-hourly data turbulent heat flux and available energy considering the heat storage term after restoration with a colorbar indicating the Bowen ratio value. Extreme Bowen ratio values have been excluded for visualization purposes, and the displayed data represents 95% of the dataset (a). Priestley-Taylor parameter (α) after restoration, where 66.59% of the values are above 1.26 (b).

IV. DISCUSSION

A. Sensible heat transfer is inhibited by the presence of a water body

The decrease in sensible heat flux and increase in latent heat flux after the tidal restoration at Hill Slough could be attributed to the energy absorbed during phase change of water within the wetland environment and, therefore, less energy being invested in increasing the air temperature. These peak values occur during summer months, characterized by higher net radiation and consequently greater available energy. During summer, the soil is warmer and the low-level jets are most intense, increasing turbulent mixing. In contrast, turbulent fluxes are minimal during winter periods (*Cuxart et al.* 2015).

B. EBC worsens significantly after tidal restoration

Before tidal restoration, the EBC nearly achieved closure. In addition, it showed improvement with the application of filters and inclusion of soil storage term. However, after tidal restoration the imbalance worsened considerably, despite the filtering and addition of the soil heat storage term. While other wetland studies report EBC $\sim$ 70% (*Stoy et al.* 2013), Hill Slough tidal wetland showed a closure of 22%, an unusually low value.

These findings underscore the site-specific nature of energy exchanges in wetlands. Since instrumentation and methodology remained consistent before and after tidal restoration, the EBC issue does not lie with the EC measuring system or instrumentation. Instead, it reveals a critical knowledge gap concerning how energy exchanges between water, soil, and atmosphere differ significantly from those occurring over dry vegetated surfaces (*Zhao and Liu* 2017).

C. Improvement of EBC with daily averaged fluxes

The significant improvement in EBC when moving from half-hourly to daily data may indicate that storage

terms are being underestimated at 30 minute time scales (*Leuning et al.* 2012). Unmeasured or inadequately measured energy storage terms are a major contributor to the lack of EBC at most sites (*Leuning et al.* 2012). In this context, water heat storage cannot be overlooked. Accounting for the entire water column resulted in unreasonably high estimates (Figure 3c), probably due to challenges in tracking water temperature, spatial temperature heterogeneity and heterogeneous bathymetry.

However, energy imbalance after tidal restoration also exists when water level is at the soil surface, indicating that water heat storage is not the sole reason for the imbalance.

The effect of lateral slow-paced energy advection, which cause energy convergence and divergence, can also be diminished by daily averaging the energy fluxes. Energy entering the soil, air and water in the morning can be returned in the afternoon and evening and be accounted for. As a result of a fluctuating water level after tidal restoration, the water is transient so the stored energy may not be released back in the same location. Discharge and temperatures of the inflow and outflow water are needed to determine this lateral heat advection carried out by tides.

Moreover, 30-minute averaging periods are insufficient to detect large-scale (several km) and slow-moving turbulent circulations caused by landscape heterogeneity, whereas considering several hours may include them (*Stoy et al.* 2013; *Charuchittipan et al.* 2014). Future studies should consider large-eddy simulations, since they can capture the contributions from secondary circulations that may be missed by shorter averaging periods (*Zhou and Li* 2019). Before tidal restoration, data did not show any improvement when averaged daily, indicating that, if there are large-scale eddies, they occur only after tidal restoration as a result of the change in energy dynamics due to the mass of water. Tidal action might create fluctuating temperature gradients and change in air flow due to changing surface relief (*Piccolo* 2019).

As a result of the resample, uncertainties due to instrument performance, EC methodology and quality control are also minimized compared to those affecting hourly fluxes (*Burba and Anderson* 2010).

D. α parameter and Bowen ratio suggest lateral heat advection after tidal restoration

A negative Bowen ratio occurs when H is negative, despite daytime expectations of positive flux from surface warming. A possible reason for negative H could be downdrafts of wind or warmer air above a cooler surface, leading to a temperature inversion. This inversion is likely caused by a warm air mass above the surface, suggesting lateral energy advection.

The poorer closure observed for negative Bowen ratios (Figure 7a) aligns with the presence of advection in these cases. An increase in negative Bowen ratio values after restoration would therefore indicate the possibility of lateral energy advection in the restored tidal wetland.

Because of some dry advection even over extensive saturated surfaces, *Priestley and Taylor* (1972) found $\alpha > 1$, with a typical value of $\alpha \approx 1.26$. This defines advection over wet surfaces as $\alpha > 1.26$, indicating an increased input of sensible heat (*Kustas and Norman* 1999). This value is empirical, but it serves as an indicator of advection under well-watered conditions (*Eichelmann et al.* 2018). After restoration, our site was expected to exhibit LE/LE_{eq} ratios near 1.26, however, 66.59% of the ratios were higher than 1.26 (Figure 7b), indicating a possible influence of advection.

This is plausible because wetland tidal restorations alter the dynamics and patterns of advection. For instance, water bodies can generate temperature differences between the restored area and neighboring urban zones, leading to unexpected advection patterns.

E. EBC ratio behaviour

Sunrise and sunset hours generate exceptionally high EBC ratios, as shown by their dependence on the zenith and azimuth angles (Figure 5). Some studies avoid the transition period by excluding from the analysis the time period covering one hour before to one hour after both sunrise and sunset due to rapid changes in solar radiation and thermal stability, which cause energy input fluctuations (*Charuchittipan et al.* 2014). However, implementing a 70-degree cutoff on the zenith only improved the EBC to 0.27, highlighting the impact of unaccounted storage terms or enhanced horizontal heat advection after tidal restoration.

EBC ratio improved with higher values of horizontal velocity (Figure 5). A larger $\overline{u}$ can enhance instability due to vertical shear in horizontal velocity, which can improve energy closure. Additionally, if there is any lateral energy advection, a high horizontal mean velocity would mitigate its impact as it would enter and exit within the 30-minute time interval. This may explain the improved EBC ratio with higher velocities (*Barr et al.* 2006).

The EBC ratio also improved with higher friction velocity $u*$ (Figure 5). *Franssen et al.* (2010) and *Barr et al.* (2006) have found that increasing $u*$ and atmospheric instability improve EBC by not underestimating to that extent turbulent heat fluxes. These conditions better fulfill Taylor's hypothesis and maintain convection, whereas low $u*$ conditions indicate low turbulence and leads to underestimation of atmospheric exchange, contributing to energy imbalance (*Sánchez et al.* 2010).

Mean daily maximum friction velocity decreased slightly from 0.7 m/s before tidal restoration to 0.5 m/s after tidal restoration, likely due to a softer surface reducing friction and limiting turbulence when water was present. This lower $u*$ after tidal restoration may prevent eddies from reaching the sensors.

Finally, as shown in Figure 6, EBC showed the worst

results under neutral conditions, marked by sunset and sunrise hours, where turbulent mixing is primarily mechanical and buoyancy is low, as found in *McGloin et al.* (2018). In contrast to this study, other studies have observed greatest EBC during near neutral atmospheric conditions, making the hypothesis that in heterogeneous landscapes, strongly unstable conditions are often characterized by larger eddies, resulting in lower EBC on average (*Franssen et al.* 2010; *Stoy et al.* 2013).

At neutral stability conditions, higher $u*$ can be attributed to the dominance of wind shear. In contrast, H and the Bowen ratio are related to buoyancy effects, being positive (negative) under unstable (stable) conditions, and approaching zero in neutral conditions.

V. CONCLUSIONS

This study explored the energy imbalance of eddy covariance measurements in a tidal restored wetland, aiming to unravel the factors contributing to this energy balance unclosure.

- Following the reintroduction of tidal activity to the wetland, LE dominated turbulent heat fluxes, contrasting with conditions before tidal restoration where H was predominant.
- The EBC after tidal restoration was found to be 0.22, lower than both typical wetlands and the before tidal restoration value of 0.90. Filtering based on u*, wind direction, and nighttime improved closure for data before tidal restoration but did not show similar effectiveness after tidal restoration.
- Daily averaging of fluxes increased the closure to 54% suggesting the influence of water heat storage, lateral heat water advection carried by tides and a possible presence of large-scale eddies.
- Lateral heat advection was identified as an additional and likely contributor to imbalance, evidenced by numerous negative Bowen ratios and Priestley-Taylor parameters exceeding 1.26.
- EBC exhibited poorer performance particularly during neutral stability conditions, which happened during sunset and sunrise, and under conditions of low $u*$ and $\overline{u}$.

This research highlighted the significance of water storage and lateral heat advection, and the challenges in accurately estimating them, in a context where energy dynamics is highly affected by tidal waters.

This thesis contributes to the advancing knowledge of tidal wetland energy dynamics emphasizing the complexities of achieving energy balance closure. By addressing these challenges, future research can enhance wetland restoration initiatives and climate change mitigation strategies.

ACKNOWLEDGMENTS

I am deeply grateful to Ariane and Carlos for dedicating their time to guide and support me throughout my thesis. Their expertise enriched my understanding in ways I could not have accomplished alone. I would like to thank Mireia for her invaluable teachings on micrometeorological concepts, which were essential for this thesis. Finally, I also want to acknowledge all my teachers and fellow students from the master's for having made this year a source of learning and joy.

REFERENCES

Arias-Ortiz, A., D. Szutu, J. Verfaillie, and D. Baldocchi, Ameriflux base us-hsm hill slough marsh, ver. 4-5., *AmeriFlux AMP, (Dataset)*, doi: https://doi.org/10.17190/AMF/189048, 2024.

Baldocchi, D. D., Assessing the eddy covariance technique for evaluating carbon dioxide exchange rates of ecosystems: past, present and future, *9*(4), 479–492, doi:10.1046/j.1365-2486.2003.00629.x, 2003.

Barr, A. G., K. Morgenstern, T. A. Black, J. H. McCaughey, and Z. Nesic, Surface energy balance closure by the eddy-covariance method above three boreal forest stands and implications for the measurement of the CO2 flux, *140*(1), 322–337, doi:10.1016/j.agrformet.2006.08.007, 2006.

Berkeley Biometeorology Lab, Equipment data at hill slough, https://biometlab.cnr.berkeley.edu/biometlab/bmetdata/equipment.php?LE=0&LL1=Hill+Slough&LV=0&LMd=0&SN=&eqlimit=Search, accessed: June 25, 2024.

Burba, G., and D. Anderson, *A Brief Practical Guide to Eddy Covariance Flux Measurements: Principles and Workflow Examples for Scientific and Industrial Applications*, doi: 10.13140/RG.2.1.1626.4161, 2010.

Charuchittipan, D., W. Babel, M. Mauder, J.-P. Leps, and T. Foken, Extension of the averaging time in eddy-covariance measurements and its effect on the energy balance closure, *152*(3), 303–327, doi:10.1007/s10546-014-9922-6, 2014.

Cui, W. T. Chui, and J. Chen, Energy balance across the eddy covariance sites (thesis), *University of Hong Kong, Pokfulam, Hong Kong SAR*, 2019.

Cuxart, J., L. Conangla, and M. A. Jiménez, Evaluation of the surface energy budget equation with experimental data and the ECMWF model in the ebro valley, *120*(3), 1008–1022, doi:10.1002/2014JD022296, 2015.

DAC, *DAC GUIDELINES ON AID AND ENVIRONMENT, Sustainable use of wetlands*, 1996.

Davidson, N., How much wetland has the world lost? long-term and recent trends in global wetland area, *Marine and Freshwater Research*, *65*, 936–941, doi:10.1071/MF14173, 2014.

Eichelmann, E., K. S. Hemes, S. H. Knox, P. Y. Oikawa, S. D. Chamberlain, C. Sturtevant, J. Verfaillie, and D. D.

Baldocchi, The effect of land cover type and structure on evapotranspiration from agricultural and wetland sites in the sacramento–san joaquin river delta, california, *256-257*, 179–195, doi:10.1016/j.agrformet.2018.03.007, 2018.

Foken, T., THE ENERGY BALANCE CLOSURE PROBLEM: AN OVERVIEW, *18*(6), 1351–1367, doi:10.1890/06-0922.1, 2008.

Foken, T., *Micrometeorology*, Springer Berlin Heidelberg, doi:10.1007/978-3-642-25440-6, 2017.

Franssen, H. J. H., R. Stöckli, I. Lehner, E. Rotenberg, and S. I. Seneviratne, Energy balance closure of eddy-covariance data: A multisite analysis for european FLUXNET stations, *150*(12), 1553–1567, doi:10.1016/j.agrformet.2010.08.005, 2010.

Heusinkveld, B. G., A. F. G. Jacobs, A. A. M. Holtslag, and S. M. Berkowicz, Surface energy balance closure in an arid region: role of soil heat flux, *122*(1), 21–37, doi:10.1016/j.agrformet.2003.09.005, 2004.

Kimball, B. A., R. D. Jackson, F. S. Nakayama, S. B. Idso, and R. J. Reginato, Soil-heat flux determination: Temperature gradient method with computed thermal conductivities, *40*(1), 25–28, doi:10.2136/sssaj1976.03615995004000010011x, 1976.

Kustas, W. P., and J. M. Norman, Evaluation of soil and vegetation heat flux predictions using a simple two-source model with radiometric temperatures for partial canopy cover, *94*(1), 13–29, doi:10.1016/S0168-1923(99)00005-2, 1999.

Lafleur, P. M., Connecting atmosphere and wetland: Energy and water vapour exchange, *2*(4), 1027–1057, doi:10.1111/j.1749-8198.2007.00132.x, 2008.

Lal, R., Carbon sequestration, *363*(1492), 815–830, doi:10.1098/rstb.2007.2185, publisher: Royal Society, 2007.

Leuning, R., E. van Gorsel, W. J. Massman, and P. R. Isaac, Reflections on the surface energy imbalance problem, *156*, 65–74, doi:10.1016/j.agrformet.2011.12.002, 2012.

Liu, X., S. Yang, J. Xu, J. Zhang, and J. a. Liu, Effects of soil heat storage and phase shift correction on energy balance closure of paddy fields, *30*(1), 39–52, doi:10.20937/ATM.2017.30.01.04, 2017.

Liu, Y., C. Weaver, and R. Avissar, Toward a parameterization of mesoscale fluxes and moist convection induced by landscape heterogeneity, *Journal of Geophysical Research*, *1041*, 19,515–19,534, doi:10.1029/1999JD900361, 1999.

Mauder, M., T. Foken, and J. Cuxart, Surface-energy-balance closure over land: A review, *177*(2), 395–426, doi:10.1007/s10546-020-00529-6, 2020.

McGloin, R., L. Šigut, K. Havránková, J. Dušek, M. Pavelka, and P. Sedlák, Energy balance closure at a variety of ecosystems in central europe with contrasting topographies, *248*, 418–431, doi:10.1016/j.agrformet.2017.10.003, 2018.

Mitra, S., R. Wassmann, and P. Vlek, An appraisal of global wetland area and its organic carbon stock, *Current Science*, *88*, 2005.

Moffett, K. B., A. Wolf, J. A. Berry, and S. M. Gorelick, Salt marsh–atmosphere exchange of energy, water vapor, and carbon dioxide: Effects of tidal flooding and biophysical controls, *46*(10), 2009WR009,041, doi:10.1029/2009WR009041, 2010.

Pendleton, L., et al., Estimating global "blue carbon" emissions from conversion and degradation of vegetated coastal ecosystems, *7*(9), e43,542, doi:10.1371/journal.pone.0043542, 2012.

Piccolo, M. C., Methods to estimate heat balance in coastal wetlands, in *Coastal Wetlands*, pp. 263–288, Elsevier, doi:10.1016/B978-0-444-63893-9.00007-1, 2019.

Pokorný, J., J. Květ, A. Rejšková, and J. Brom, Wetlands as energy-dissipating systems, *Journal of industrial microbiology biotechnology*, *37*, 1299–305, doi:10.1007/s10295-010-0873-8, 2010.

Priestley, C. H. B., and R. J. Taylor, On the assessment of surface heat flux and evaporation using large-scale parameters, section: Monthly Weather Review, 1972.

Reynolds, O., IV. on the dynamical theory of incompressible viscous fluids and the determination of the criterion, *186*, 123–164, doi:10.1098/rsta.1895.0004, publisher: Royal Society, 1895.

Schedlbauer, J. L., S. F. Oberbauer, G. Starr, and K. L. Jimenez, Controls on sensible heat and latent energy fluxes from a short-hydroperiod florida everglades marsh, *411*(3), 331–341, doi:10.1016/j.jhydrol.2011.10.014, 2011.

Stoy, P. C., et al., A data-driven analysis of energy balance closure across FLUXNET research sites: The role of landscape scale heterogeneity, *171-172*, 137–152, doi:10.1016/j.agrformet.2012.11.004, 2013.

Stull, R. B., *An Introduction to Boundary Layer Meteorology*, Springer Science & Business Media, google-Books-ID: eRRz9RNvNOkC, 1988.

Sánchez, J. M., V. Caselles, and E. M. Rubio, Analysis of the energy balance closure over a FLUXNET boreal forest in finland, *14*(8), 1487–1497, doi:10.5194/hess-14-1487-2010, publisher: Copernicus GmbH, 2010.

Twine, T. E., W. P. Kustas, J. M. Norman, D. R. Cook, P. R. Houser, T. P. Meyers, J. H. Prueger, P. J. Starks, and M. L. Wesely, Correcting eddy-covariance flux underestimates over a grassland, *103*(3), 279–300, doi:10.1016/S0168-1923(00)00123-4, 2000.

Webb, E. K., G. I. Pearman, and R. Leuning, Correction of flux measurements for density effects due to heat and water vapour transfer, *106*(447), 85–100, doi:10.1002/qj.49710644707, 1980.

Zhao, X., and Y. Liu, Phase transition of surface energy exchange in china's largest freshwater lake, *244-245*, 98–110, doi:10.1016/j.agrformet.2017.05.024, 2017.

Zhou, Y., and X. Li, Energy balance closures in diverse ecosystems of an endorheic river basin, *274*, 118–131, doi:10.1016/j.agrformet.2019.04.019, 2019.

VI. APPENDIX

A. Windrose of the study site

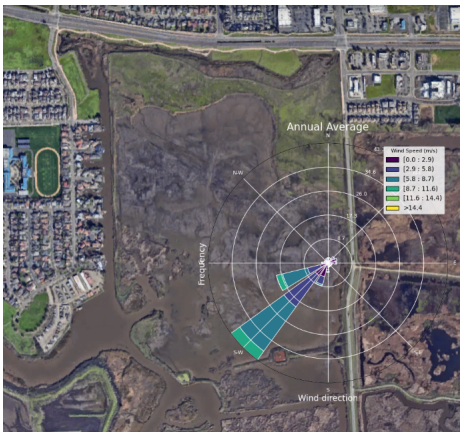

Figure 8: Windrose showing annual average wind speed and direction in an aerial view (Google Earth) of Hill Slough tidal wetland.

B. Evolution of various variables in the study site

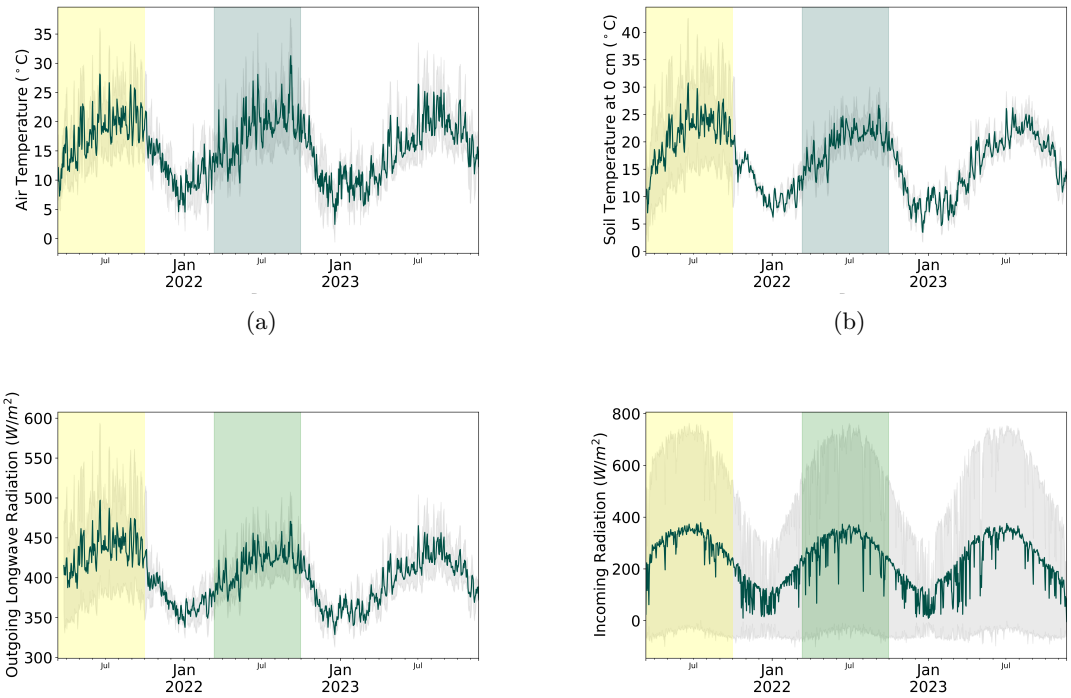

Figure 9: Evolution of daily averaged air temperature (a), soil temperature at 0 cm (b), outgoing long-wave radiation (c), and incoming radiation (d). The grey background indicates the standard deviation, the yellow band represents the studied period before tidal restoration, and the green band represents the studied period after tidal restoration.